PROCEEDINGS OF SCIENCE

# Signals of the first order phase transition?

**Jørgen Randrup**[*†]

*Nuclear Science Division, Lawrence Berkeley National Laboratory, Berkeley, California, USA*

The phase diagram of strongly interacting matter presents a focal point for current high-energy nuclear physics as several facilities are preparing to mount experimental programs devoted to the search for the expected first-order phase transition and the associated critical point. For this effort to succeed, it is important to develop suitable dynamical models that can be used to test candidate signals and provide a framework for the interpretations of the data.

Starting with a brief reminder of the thermodynamics relevant for first-order phase transitions, we illustrate the intricacies of the associated phase diagrams for the simple cases of either zero or one conserved charge. We then turn to the phase trajectories of the hot and dense matter formed in a high-energy collision. The generic features suggest that there is an optimal range of collision energies within which the system spends the longest time inside the thermodynamically unstable phase-coexistence region and thus is most likely to undergo a phase separation.

Subsequently, within the general framework of collective dynamics in many-body systems, we elucidate how the presence of a phase transition induces a transient enhancement of the mode fluctuations, and the more so the further the system ventures into the unstable region.

Finally, we briefly discuss the spinodal clumping that may occur if the expansion dynamics drives the bulk matter into the spinodal region of instability. We review both kinematic and chemical correlation observables that exhibit a sensitivity to such a clumping and may therefore be useful as signals of that phenomenon and thus help to identify the first-order transition.

*Critical Point and Onset of Deconfinement - 4th International Workshop*
*July 9 - 13, 2007*
*Darmstadt, Germany*

[*]Invited speaker.

[†]E-mail: Randrup@LBL.gov

 

PoS(CPOD07)006

## 1. Introduction

Several years of vigorous research with high-energy nuclear collisions have provided compelling evidence for the existence of a new phase of matter which has been tentatively identified as the expected quark-gluon plasma. A central goal of the field is now to investigate this deconfined phase and, in particular, to explore the phase structure of strongly interacting matter.

While the confinement phase transformation appears to be a crossover in baryon-poor matter (which has been most extensively studied so far), it is expected to become of first order at sufficiently high baryochemical potential. The prospect of establishing evidence of this first-order phase transition and identifying the associated critical point has stimulated a rapid growth of interest in hot and baryon-dense matter and several facilities around the world are being prepared to address this hitherto unexplored physics area [1, 2, 3]

There are numerous significant challenges associated with this venture. For one thing, we do not yet have quantitative theoretical predictions of how the phase diagram should look, so the experimentalists need to prepare for a broad range of possibilities. Furthermore, as always in heavy-ion physics, the success of the experimental effort depends on the identification of measurable and informative observables and this, in turn, requires the availability of suitable simulation models with the help of which the robustness of proposed signals can be tested and effective data analyzes devised. Unfortunately, it is particularly difficult to develop such models for the phase region of primary interest where the effective degrees of freedom change from partonic to hadronic. We discuss here key features of such a first-order phase transition with a view towards developing suitable signal observables.

## 2. Thermodynamics reminder

We start by a reviewing the thermodynamics relevant in connection with a first-order phase transition. In this discussion, the term "thermodynamics" refers to the statistical dynamics of systems that are spatially uniform (*i.e.* translationally invariant) and sufficiently large that finite-size effects are insignificant.

Consider now such a system of volume $V$ and let its total energy be $E = V\varepsilon$, where $\varepsilon = E/V$ is the energy density. In general the system may contain certain amounts of conserved charges, which we here shall examplify by the "particle number" $N = V\rho$ (in the nuclear context it may be thought of as the *net* baryon number), with $\rho = N/V$ being the corresponding net charge density.

The key thermodynamic quantity is the associated entropy $S(E,N,V) = V\sigma(\varepsilon,\rho)$, with the entropy density $\sigma = S/V$, whose derivatives yield the thermodynamic parameters $T$, $\mu$, and $p$:

$$\partial_E S(E,N,V) = \frac{1}{T} = \beta(\varepsilon,\rho) = \partial_\varepsilon \sigma(\varepsilon,\rho)\,, \tag{2.1}$$

$$\partial_N S(E,N,V) = -\frac{\mu}{T} = \alpha(\varepsilon,\rho) = \partial_\rho \sigma(\varepsilon,\rho)\,, \tag{2.2}$$

$$\partial_V S(E,N,V) = \frac{p}{T} = \pi(\varepsilon,\rho) = \sigma(\varepsilon,\rho) - \beta(\varepsilon,\rho)\varepsilon - \alpha(\varepsilon,\rho)\rho\,. \tag{2.3}$$

In the thermodynamic limit ($V \to \infty$) the volume plays no role and the thermodynamic properties can be expressed solely in terms of the densities $\varepsilon$, $\rho$, and $\sigma$, as shown above on the right.

The conditions for *thermodynamic coexistence* of two such systems in contact can be obtained by requiring that the total entropy $S_{1+2} = S_1 + S_2$ be stationary, $\delta S_{1+2} \doteq 0$, for arbitrary conserving variations in energy ($\delta E_1 + \delta E_2 = 0$), charge ($\delta N_1 + \delta N_2 = 0$), and volume ($\delta V_1 + \delta V_2 = 0$). This yields the conditions $\partial_{E_1} S_1 \doteq \partial_{E_2} S_2$ (implying $T_1 = T_2$), $\partial_{N_1} S_1 \doteq \partial_{N_2} S_2$ (implying $\mu_1 = \mu_2$), and $\partial_{V_1} S_1 \doteq \partial_{V_2} S_2$ (implying $p_1 = p_2$). These conditions can be visualized as the requirement that the tangents of the entropy density $\sigma(\varepsilon,\rho)$ at the two coexisting phase points $(\rho_1,\varepsilon_1)$ and $(\rho_2,\varepsilon_2)$ be identical: $\sigma(\varepsilon_1,\rho_1) + \beta_1(\varepsilon-\varepsilon_1) + \alpha_1(\rho-\rho_1) \doteq \sigma(\varepsilon_2,\rho_2) + \beta_2(\varepsilon-\varepsilon_2) + \alpha_2(\rho-\rho_2)$.

Furthermore, *thermodynamic stability* exists when the second variation of the entropy yields a lower value, $\delta^2 S_{1+2} < 0$. This requirement translates into the demand that the entropy density be a concave function, *i.e.* the eigenvalues of its curvature matrix $\{\partial_x \partial_{x'} \sigma\}$ must all be negative. Thus the occurrence of a convex anomaly in $\sigma(\varepsilon,\rho)$ signals the existence of a first-order phase transition, *i.e.* two different manifestations of the system that may coexist thermodynamcially.

### 2.1 Simplest example: No conserved charges

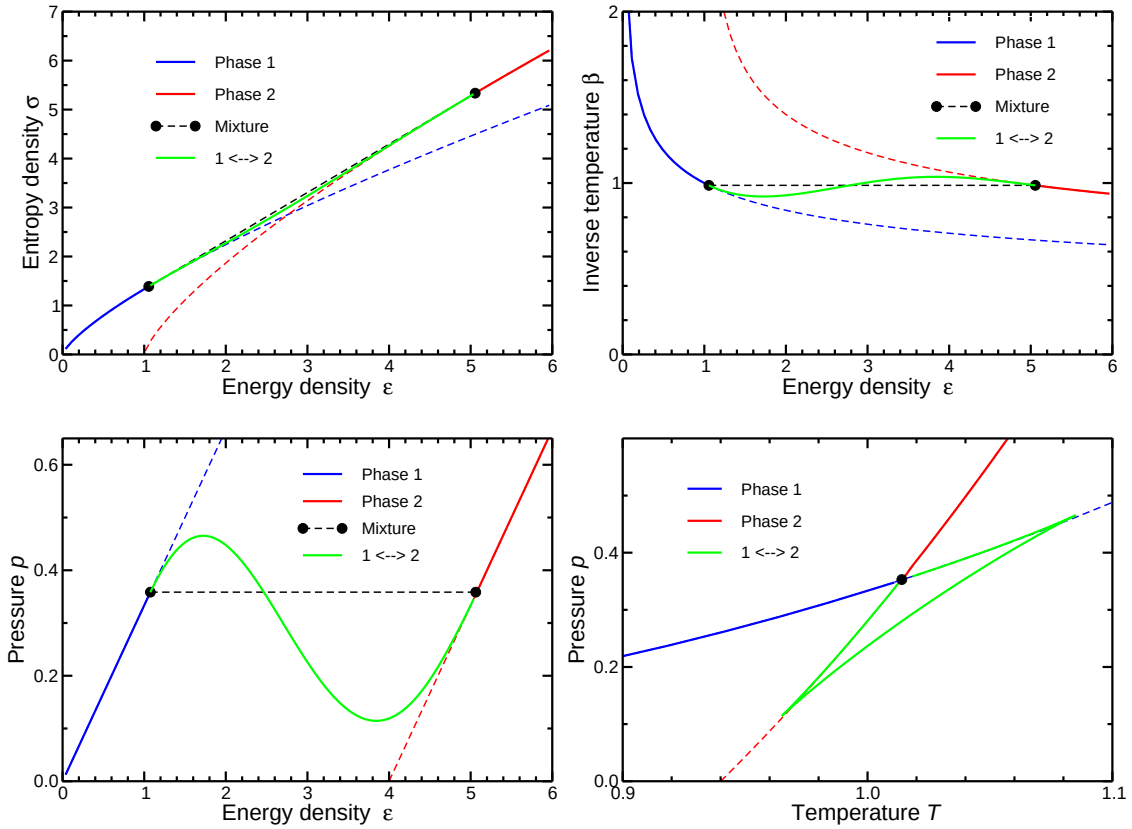


**Figure 1:** First-order phase transition without conserved charges: When the entropy density $\sigma(\varepsilon)$ has a convex anomaly there is a common tangent connecting the two coexistence points that have the same values of $T$ and $p$ (*upper left*). The slope of $\sigma(\varepsilon)$ is the inverse temperature $\beta(\varepsilon)$ which is then non-monotonic and it increases through the (spinodal) interval of the convexity (*upper right*). The pressure is also non-monotonic and decreases through the spinodal region (*lower left*). The resulting equation of state $p(T)$ then executes a complicated behavior as the phase-coexistence region of $\varepsilon$ is traversed (*lower right*).

It is instructive to first consider the simplest situation when there are no conserved charges. The key function is then $\sigma(\varepsilon)$ and we have $\beta(\varepsilon) = \partial_\varepsilon \sigma(\varepsilon)$ and $\pi(\varepsilon) \equiv p(\varepsilon)/T(\varepsilon) = \sigma(\varepsilon) - \beta(\varepsilon)\varepsilon$. The presence of a convex anomaly in $\sigma(\varepsilon)$ is illustrated in Fig. 1 which brings out the fact the thermodynamic variables $T(\varepsilon)$ and $p(\varepsilon)$ are non-monotonic functions of the mechanical control variable $\varepsilon$ in the phase-coexistence region, causing the corresponding inverse functions to be triple-valued and resulting in a multilayered appearance of the thermodynamic equation of state $p(T)$.

### 2.2 One conserved charge: nuclear matter

We further illustrate the phase-transition thermodynamics by considering an idealized model with one conserved charge that resembles the familiar case of iso-symmetric nuclear matter. It is defined in Fig. 2 which also depicts the associated equation of state.

Ideal classical gas in a mean field

$$\Omega(E,N,V) = \frac{1}{N!}\frac{V^N}{\Gamma(\frac{3}{2}N)}\left(\frac{2\pi m}{h^2}\right)^{\frac{3}{2}N}[E - Vw(\rho)]^{\frac{3}{2}N-1}$$

$$\sigma(\epsilon,\rho) \equiv \frac{1}{V}\ln\Omega(V\epsilon, V\rho, V) = \rho[s_0 - \tfrac{5}{2}\ln\rho + \tfrac{3}{2}\ln\tfrac{2}{3}(\epsilon - w(\rho))]$$

$$\beta(\epsilon,\rho) = \tfrac{3}{2}\frac{\rho}{\epsilon - w(\rho)} \quad\leftrightarrow\quad \rho T(\epsilon,\rho) = \tfrac{2}{3}[\epsilon - w(\rho)]$$

$$w(\rho) = m\rho - C\frac{\rho^2}{\rho_0^2} + C\frac{\rho^3}{\rho_0^3} \;:\; m = 1\,,\ \rho_0 = 1\,,\ C = 5$$

$$p_T(\rho) = \rho T + \rho\partial_\rho w(\rho) - w(\rho) = \rho T - C\frac{\rho^2}{\rho_0^2} + 2C\frac{\rho^3}{\rho_0^3}$$

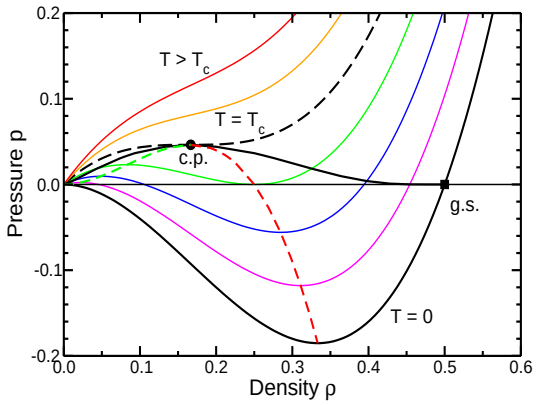


**Figure 2:** Schematic model of nuclear matter: *Left:* Description of the model which considers classical particles in a density-dependent mean field. *Right:* The associated equation of state $p_T(\rho)$ is depicted by plotting the pressure plotted as a function of density $\rho$ for a succession of fixed temperatures $T$. The solid curve between the vacuum and the ground state goes through the phase coexistence points, while the dashed curves delineate the low (green) and high (red) density spinodal boundaries, joining at the critical point.

It is instructive to consider the phase diagram in various representations, as done in Fig. 3. In the mechanical $(\rho,\varepsilon)$ representation all features are visible on a single sheet since the thermodynamic functions are all single-valued everywhere; the accessible part of the phase diagram is bounded from below by the zero-temperature energy density $\varepsilon_{T=0}(\rho)$. Furthermore, phase trajectories resulting from dynamical expansions have a simple appearance.

In the $(\rho,T)$ diagram the entire upper half plane is accessible and coexisting phase points are joined by horizonthal lines; dynamical trajectories tend to be well-behaved here as well. By contrast, the $(\mu,\varepsilon)$ representation yields a rather complicated phase diagram that requires multiple sheets and the dynamical phase trajectories are correspondingly complicated.

In the familiar $(\mu,T)$ diagram the phase coexistence partners coincide and the entire phase coexistence region lies on intermediate sheets that are usually not displayed. This representation is therefore particularly inconvenient for the discussion of phase transition dynamics. This problem is well illustrated by the expansion phase trajectories which cross the phase transition line three times and thus exhibit a zig-zag behavior as the phase coexistence region is being traversed.

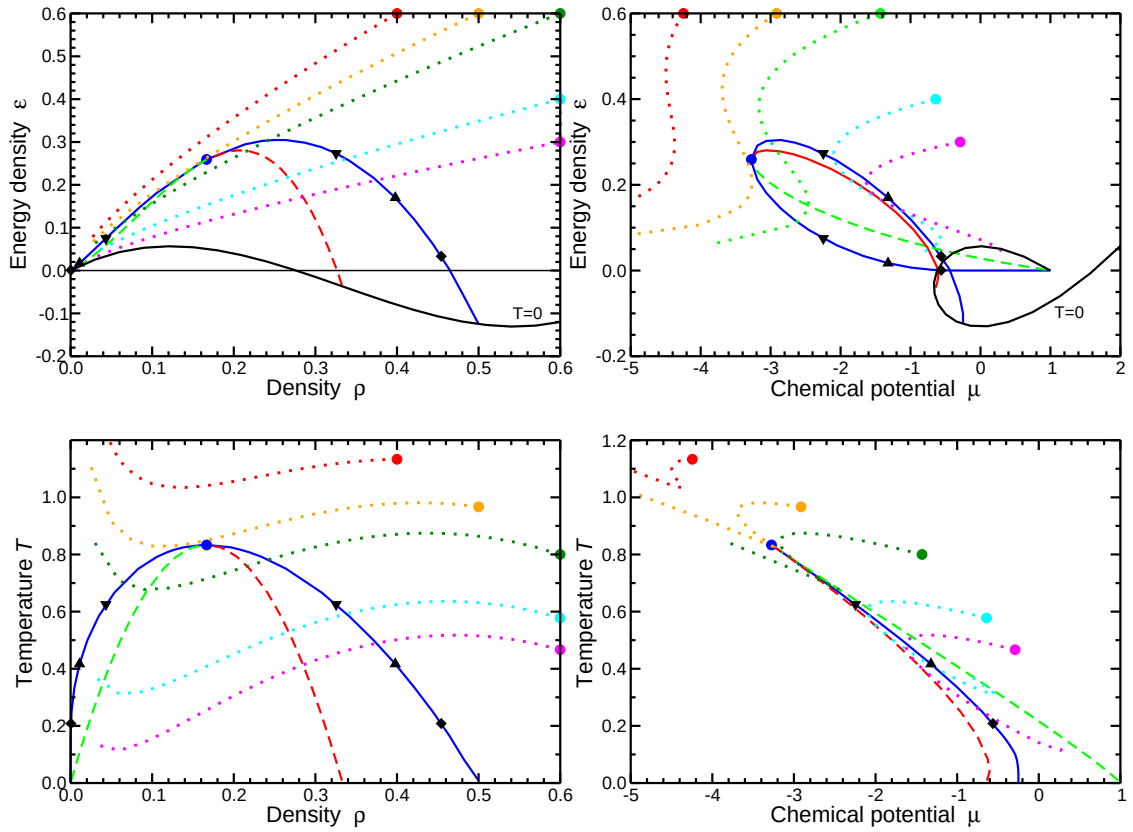


**Figure 3:** Various representations of the phase diagram for a liquid-gas type system with one conserved charge. Starting from the basic mechanical representation $(\rho,\varepsilon)$ (*upper left*), either density may be replaced by the corresponding thermodynamic variable, yielding either $(\mu,\varepsilon)$ (*upper right*) or $(\rho,T)$ (*lower left*) phase diagrams, and ultimately the $(\mu,T)$ representation familiar from text books (*lower right*). Also shown are the phase trajectories resulting from (approximately) isentropic expansions of uniform matter.

## 3. Dynamical phase trajectories for nuclear collisions

The prospects for probing the phase structure of hot and dense matter with high-energy nuclear collisions depends of which parts of the phase diagram are being visited during the dynamical evolution. This can be elucidated by considering the evolving densities $\rho(t)$ and $\varepsilon(t)$ together by plotting the dynamical trajectory in the $\rho-\varepsilon$ phase plane, as done in Ref. [4], see Fig. 4 (*left*). That study demonstrated that a number of quite different dynamical models yield very similar results for these quantities. We may therefore extract certain generic features, illustrated in Fig. 4 (*right*).

Obviously, the lowest collision energies are insufficient to bring the system near the phase coexistence region. Generally, as the collision energy is increased, the phase trajectories penetrate into ever larger compressions and excitations and the (nearly isentropic) expansion paths steepen. Therefore, there will be a certain "critical" collision energy for which the expansion trajectory will pass right through the critical point. Above this energy the dynamical trajectory will entirely miss the phase coexistence region and such "supercritical" collision energies would seem rather unlikely to provide direct signals of the first-order transition.

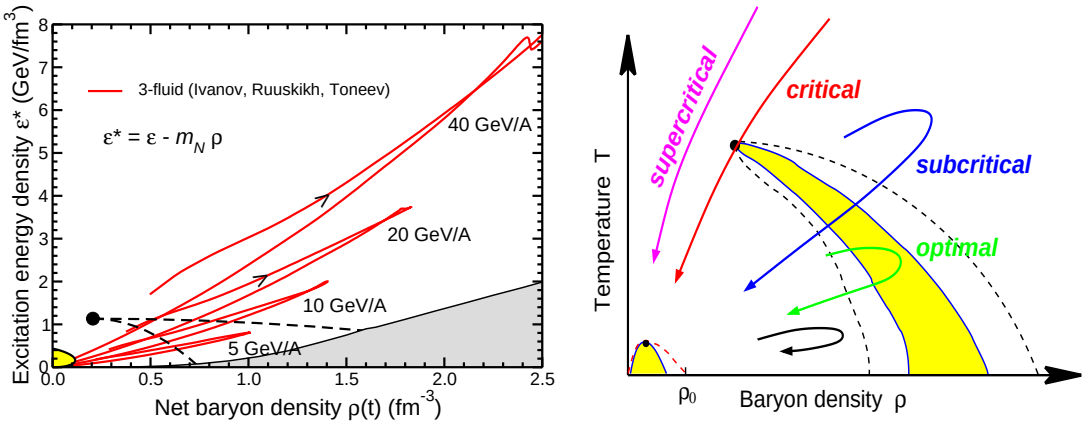


**Figure 4:** Dynamical phase trajectories. *Left:* Time evolution of the mechanical phase point $(\rho(t), \varepsilon^*(t))$ extracted at the center of a head-on gold-gold collision as calculated in the 3-fluid model (from Ref. [4]). *Right:* Sketch of the associated generic features as a sweep is made in the collision energy.

On the other hand, there is an entire range of relatively low collision energies for which the phase trajectories penetrate into but not beyond the phase coexistence region. The bulk of the system then spends a maximal amount of time in the thermodynamcially unstable phase region. These circumstances may be optimal for a phase separation to develop. Such a macroscopic reorganization into a phase mixture renders the system highly irregular and is expected to lead to anomalously large fluctuations in various observables (see later).

Unfortunately, it is not yet possible to make a precise prediction of the corresponding "optimal' collision energies, partly because of the uncertainties inherent in the dynamical collision simulations, but mostly because the lack of sufficiently realistic calculations of the phase diagram. Because of this situation, theory can only provide qualitative guidance and experimental data on the phase structure are urgently needed.

## 4. Collective dynamics near a critical point

There is currently some debate about the dynamical behavior of collective modes in the neighborhood of a critical point and we wish to illuminate the issue within a schematic model that has the relevant characteristic features.

Following Ref. [5], we consider the dynamical evolution of a general many-body system after its collective modes have been identified and the corresponding equations of motion have been linearized. These collective modes are labeled by the index $\nu$ and the associated quantum amplitudes are $\{A_\nu\}$. The time evolution of $A_\nu$ is governed by the following equation of motion,

$$\frac{d}{dt}A_\nu(t) \;=\; -i\omega_\nu A_\nu(t) + B_\nu(t)\;,\;\; \prec B_\nu(t)B^*_\mu(t')\succ \;=\; 2\mathscr{D}_{\nu\mu}\delta(t-t')\;, \tag{4.1}$$

where the coupling of the collective modes to the residual system is accounted for by the stochastic terms $\{B_\nu\}$ which we here assume to be diagonal and Markovian (the expectation value is taken over the considered ensemble of systems).

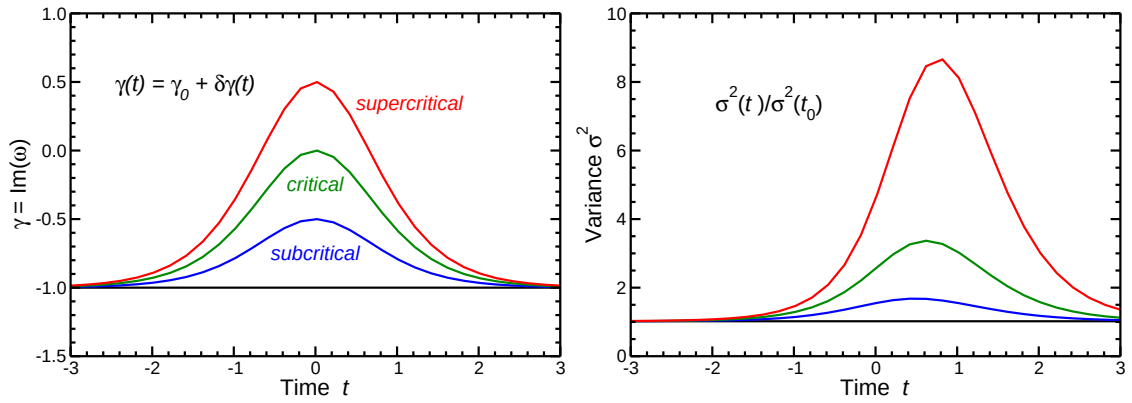


**Figure 5:** Dynamics near a critical point. *Left:* The prescribed time evolution of the imaginary part $\gamma_\nu$ of the eigenfrequency of a particular mode in four different scenarios: equilibrium, $\gamma(t)=\gamma_0$ (black), subcritical, $\gamma_{\max}<0$ (blue), critical, $\gamma_{\max}=0$ (green), and supercritical, $\gamma_{\max}>0$ (red). *Right:* The resulting evolution of the induced transient agitation of the mode as measured by the variance of the associated amplitude $A_\nu$.

The eigenfrequency is generally complex, $\omega_\nu=\varepsilon_\nu+i\gamma_\nu$. When the mode is stable, $\gamma_\nu$ is negative and its magnitude represents the damping width due to the interaction with the residual system. Conversely, the frequency is purely imaginary when the mode is unstable at the mean-field level. Generally, the imaginary part of the frequency is the difference between the damping width and the growth rate and it may therefore become positive, thus producing an exponential development of $A_\nu$. We now illustrate this by considering the fluctuations of the amplitudes $A_\nu(t)$.

While we may generally study the two-time correlation matrix, $\sigma_{\nu\mu}(t_1,t_2)\equiv\prec A_\nu(t_1)A^*_\mu(t_2)\succ$, we focus here on just the diagonal elements of the same-time correlation $\sigma^2_\nu(t)=\prec A_\nu(t)A^*_\nu(t)\succ$, which is a convenient measure of the degree of agitation of the mode. This quantity evolves according to a simple feed-back equation of motion [5],

$$\frac{d}{dt}\sigma^2_\nu(t) \;=\; 2\mathscr{D}_\nu \;+\; 2\gamma_\nu\sigma^2_\nu(t)\;, \tag{4.2}$$

where the source term $\mathscr{D}_\nu$ expresses the continual noisy input from the residual system. When $\gamma_\nu$ is negative, the feed-back term suppresses these disturbances and thus ensures that the appropriate equilibrium variance is approached. $\sigma^2_\nu(t-\to\infty)=-\mathscr{D}_\nu/\gamma_\nu$. On the other hand, the feed-back term amplifies disturbances when $\gamma_\nu$ is positive. These features are evident in the general solution,

$$\sigma^2_\nu(t) \;=\; \left[2\mathscr{D}_\nu\int_{t_i}^{t}\mathrm{e}^{2\Gamma_\nu(t')}dt'+\sigma^2_\nu(t_i)\right]\mathrm{e}^{-2\Gamma_\nu(t)}\;,\;\; \Gamma_\nu(t)\equiv\int_{t_i}^{t}\gamma_\nu(t')\,dt'\;. \tag{4.3}$$

We now emulate the effect of the dynamics near the critical point by prescribing the time evolution $\gamma(t)=\gamma_0+\delta\gamma(t)$. Starting in equilibrium with $\gamma(t)=\gamma_0<0$, the mode responds to the temporary increase $\delta\gamma(t)$ caused by the instability of the system, as illustrated in Fig. 5.

We first consider a subcritical scenario where the dynamical phase trajectory passes by the critical point without entering the phase-coexistence region. The mode then remains stable but the temporary decrease of $|\gamma|$ causes the instantaneous equilibrium variance to become temporarily larger; the dynamical readjustment of the variance to this change is delayed by the relaxation time.

When the dynamics takes the system right through the critical point, the value of $\gamma$ reaches zero, but for a moment only. Therefore, even though the equilibrium fluctuations diverge for $\gamma = 0$, the dynamically determined fluctuations remain well behaved (and subsequently subside again).

Finally, the supercritical phase trajectories pass through the spinodal phase region where $\gamma > 0$ and spontaneous amplitude amplification would occur in static matter. Nevertheless, again because of the finite time spent in the unstable region, the resulting fluctuations remain finite but they (temporarily) reach values that are still larger than those attained for the critical trajectory.

It thus appears than one would generally expect that a sweep from subcritical to supercritical trajectories would show a relatively sudden (but transient) enhancement of the fluctuations as the critical trajectory is being approached, followed by further (and even stronger) enhancement as the supercritical region is entered. This feature is expected to be rather generic and it may therefore form the basis for devising suitable experimental signals. It should of course be kept in mind that when the fluctuations grow sufficiently large, the system will leave the linear regime and the trajectories will branch into channels that are qualitatively different from one another. While this non-linear behavior renders the problem more difficult to treat theoretically, it may well be helpful for the experimental identification of the phase transition and the associated critical point.

## 5. Signals of spinodal clumping

If the deconfinement phase transformation of strongly interacting matter is of first-order *and* the expanding deconfined matter created in a high-energy nuclear collision enters the corresponding region of phase coexistence, a spinodal phase separation might occur (especially if the overall expansion is sufficiently slow compared to the most rapid instability growth rates). The matter would then condense into a number of separate blobs, each with its own collective flow and strangeness contents. These features may form the basis for the development of suitable diagnostic observables.

In the following, we discuss certain specific observable consequences of such a phase decomposition. For this purpose, we employ a schematic model in which the system breaks up into entirely independent blobs which proceed to hadronize statistically. The blob sizes, positions, and flow velocities are sampled from specified distributions. However, there is yet no account taken of post-hadronization interactions and decays; these processes would generally be expected to erode the signals and it would clearly be interesting to incorporate them into the simulation studies.

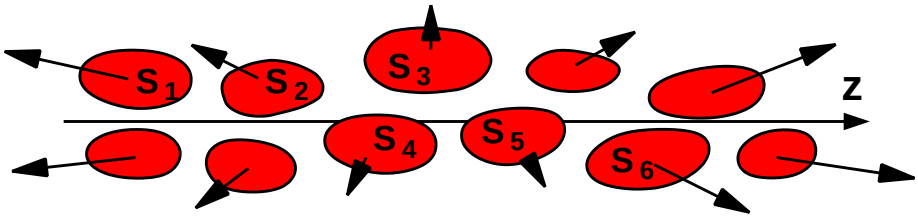


**Figure 6:** Schematic picture of spinodal clumping in a high-energy nuclear collision: The rapid longitudinal expansion drives the bulk matter into the phase coexistence region. The spinodal instabilities may then amplify density irregularities and cause the system to form individual clumps of quark-gluon plasma, each of which is endowed with its own flow velocity and a (stochastic) amount of net strangeness.

### 5.1 Kinematic signals of clumping

A clumping of the expanding system is expected to affect the kinematic correlations between the resulting hadrons. One simple kinematic observable that may be affected by a clumping is the rapidity difference between two hadrons, $|y_1 - y_2|$. Because heavy hadrons are affected less by the thermal smearing, it may be advantageous to limit the considerations to baryons. Fig. 7 (*left*) shows the calculated two-proton correlation with regard to either the ordinary longitudinal rapidity or the rapidity associated with their three-dimensional relative motion, $y_{12} = \ln[\gamma_{12} + \sqrt{\gamma_{12}^2 - 1}]$ (with $\gamma_{12} = p_1 \cdot p_2 / m_1 m_2$), which yields a significantly stronger signal [6].

Since there are several sources of two-particle correlations, it is advantageous to consider kinematic correlations between $N > 2$ particles. A particularly convenient and instructive $N$-body correlation observable is the internal kinetic energy per particle, $\kappa_N\{p_n\}$, for a group of $N$ simultaneously observed particles having four-momenta $\{p_n\}$ [6]. When the $N$-body momentum distribution is clumped, the sampling of $\kappa_N$ will yield an enhancement around the thermal kinetic energy in the individual source, relative to what would occur for a structureless distribution. In order to bring out this signal, one may compare the correlated distribution $P(\kappa_N)$, obtained by sampling all the $N$ particles from the same event, with the corresponding uncorrelated distribution $P_0(\kappa_N)$ obtained by sampling $N$ different events. This yields the reduced correlation function, $C_N(\kappa_N) \equiv P(\kappa_N)/P_0(\kappa_N) - 1$, which is illustrated in Fig. 7 (*right*).

The correlation signal grows more prominent as $N$ is increased, because it becomes increasingly unlikely that $N$ momenta sampled from a structureless distribution would all be nearly similar, and the higher-order correlations become progressively more effective in discriminating between various dynamical mechanisms. However, since the signal receives its support from a suppressed region of the $N$-body phase space, the required counting statistics increases rapidly with $N$, thus presenting a practical limit to the order of correlation that can be addressed with a given set of data. This basic feature illustrates the importance of having sufficiently large event samples for the identification of a conclusive correlation signal.

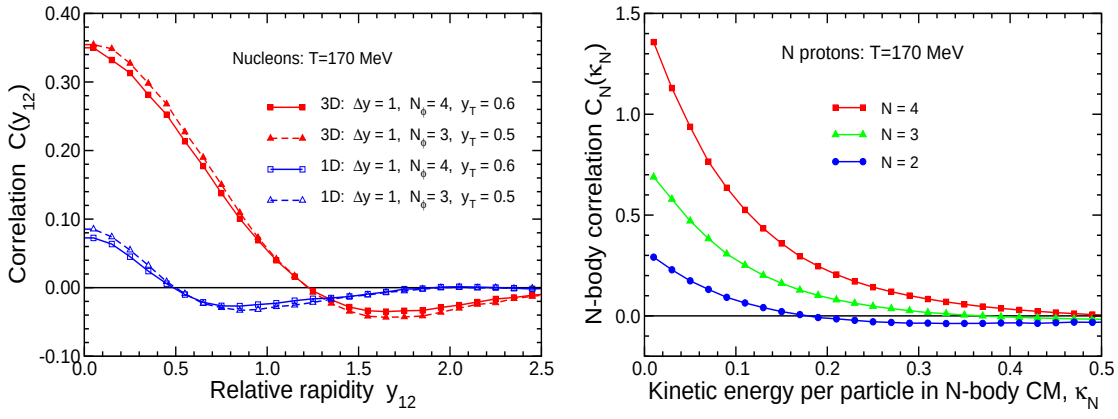


**Figure 7:** Kinematic signals of clumping (from Ref. [6]). *Left:* The 1D and 3D two-proton rapidity correlation functions in a variety of clumping scenarios. *Right:* The correlation function function for $N = 2, 3, 4$ protons expressed as the enhancement of the internal kinetic energy per particle of the observed $N$ protons.

### 5.2 Chemical signals of clumping

Since the particular net strangeness trapped in a given spinodal blob would remain approximately conserved during its further evolution, the resulting hadrons will exhibit an enhanced degree of strangeness fluctuation, relative to a statistical emisson from the overall system [7]. [This is qualitatively easy to understand since the requirement that the total strangeness in a given blob be non-zero necessarily puts a lower bound on the number of strange hadrons produced, whereas no such bound exists when the total strangeness vanishes.] As a result of this elementary effect of clumping, suitable strangeness-related observables may be useful signals of a phase separation.

For a source having a significant net baryon density, where a first-order transition is expected, Fig. 8 (*left*) illustrates the dependence of the fluctuation of the $K^+/\pi^+$ yield ratio on the overall baryochemical potential, compared with that would result if the strangeness of each blob were fixed to zero or if a grand canonical treatment were employed. The effect is seen to become significant for large values of the chemical potential.

But there are two opposing effects: The fluctuations are generally enhanced by the fact that the plasma has more active degrees of freedom, while they are suppressed by the expansion which increases the available hadronic volume. The net effect is illustrated in Fig. 8 (*right*) which shows the dependence on the $K^+/\pi^+$ fluctuation on the degree of expansion between the formation of the plasma blob (which is assumed to occur at $T = T_q$ and $V = V_q$) to the effective volume at the time of hadronization canonical emission (at $T = T_h$ and $V = V_h = \chi V_q$). It is therefore to be expected that a smaller degree of expansion will yield a larger degree of strangeness fluctuation, as is indeed borne out in the illustration. In fact, it can be seen that the value $\chi = 3$ used in [7] (*left panel*) is particularly unfavorable with regard to the enhancement of strangeness fluctuations and even a modestly smaller expansion ratio would yield a significantly larger fluctuation effect.

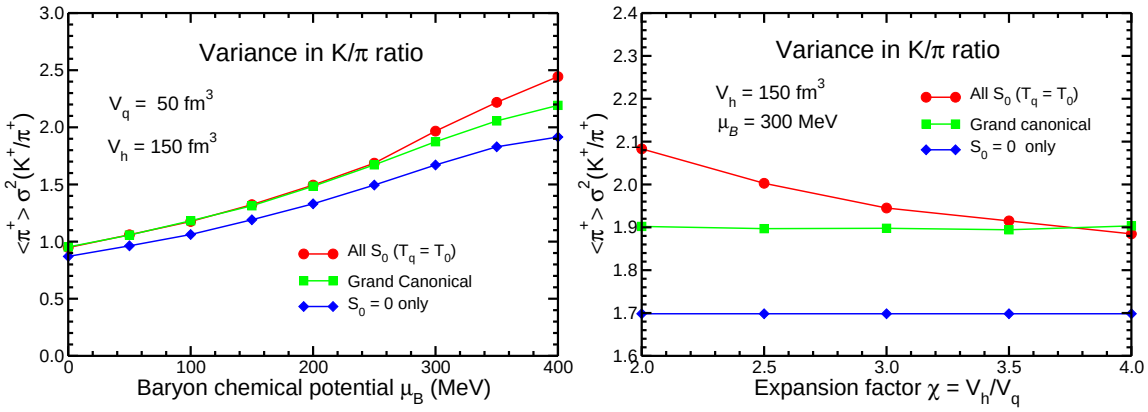


**Figure 8:** Signals of strangeness trapping (from Ref. [7]): *Left:* The variance of the $K^+/\pi^+$ ratio as a function of the baryochemical potential $\mu_B$ and an expansion factor of $\chi = 3$, for three different statistical treatments of the of strangeness $S_0$ within each blob: grand-canonical equilibrium (green), canonical equilibrium with $S_0 = 0$ (blue), and canonical equilibrium with $S_0$ having been determined by the (stochastic) number of $s$ and $\bar{s}$ quarks it contains at the time of its formation, $S_0 = N_{\bar{s}} - N_s$. *Right:* The variance of the $K^+/\pi^+$ ratio for $\mu_B = 300$ MeV as a function of the assumed expansion factor $\chi = V_h/V_q$.

## 6. Concluding remarks

The development of robust signals of the first-order confinement phase transition is still in its infancy and presents many interesting challenges.

In particular, attempts to learn about the thermodynamics of strongly interacting matter by means of nuclear collision experiments have to overcome significant obstacles because the systems are small in size, non-uniform in space, rapidly evolving in time, and may not achieve even local equilibrium. Due to these inherent features, the connection between the collision observables and the underlying thermodynamical properties is not simple. Indeed, it is necessary to rely on dynamical transport models with which the entire collision process can be simulated. Such models are particularly difficult to develop when phase transitions are present because the effective degrees of freedom change from partonic to hadronic.

Nevertheless, even in the absence of quantitatively reliable calculations, a number of general expectations emerge: As the collision energy is being lowered from the current RHIC regime, the generated compression and excitation decreases as well, as does the slope of the $(\rho,\varepsilon)$ phase trajectory associated with the expansion stage. There should, therefore, be a cerain "critical" collision energy for which the expansion phase trajectory goes right through the critical point. As this collision energy is approached from above, a number of observables are expected to acquire ever larger fluctuations. If these fluctuations survive the subsequent hadronic gas expansion they may be used to signal the onset of the phase transition (and hence the approximate location of the critical point). It is important to recognize that the fluctuations are generally expected to keep increasing even further at subcritical collision energies where the phase trajectory is being driven through the thermodynamcially unstable phase coexistence region.

Inside the spinodal part of the phase coexistence region, a bulk system seeks to phase separate and such a clumping may be particularly useful as a phase-transition signal [8]. One may expect that the optimal conditions for a phase separation to develop would occur when the bulk of the collision system spends the longest time inside the unstable region and this is expected to happen within a range of relatively low collision energies, starting somewhat above the lowest collision energy for which the phase coexistence boundary can be still reached.

## References

[1] P. Senger, *J. Phys.* **G30** (2004) S1087

[2] G.S.F. Stephans, *J. Phys.* **G32** (2006) S447

[3] A. I. Malakov, A.N. Sissakian, A.S. Sorin and S. Vokal, Phys. Part. Nucl. **38** (2007) 407

[4] I. Arsene, L. Bravina, W. Cassing, Yu. Ivanov, A. Larionov, J. Randrup, V. Ruuskikh, V. Toneev, G. Zeeb and D. Zschiesche, Phys. Rev. **C75** (2007) 34902

[5] M. Colonna, Ph. Chomaz and J. Randrup, Nucl. Phys. **A567** (1994) 637

[6] J. Randrup, *J. Heavy Ion Phys.* **22** (2005) 69

[7] V. Koch, A. Majumder and J. Randrup, Phys. Rev. **C72** (2005) 64903

[8] M. Colonna, Ph. Chomaz and J. Randrup, Phys. Reports **389** (2004) 263